Modified Dual-Energy Algorithm for Calcified Plaque Removal: Evaluation in Carotid Computed Tomography Angiography and Comparison With Digital Subtraction Angiography

Mannil, Manoj ; Ramachandran, Jaychandran ; Vittoria de Martini, Ilaria ; Wegener, Susanne ; Schmidt, Bernhard ; Flohr, Thomas ; Krauss, Bernhard ; Valavanis, Antonios ; Alkadhi, Hatem ; Winklhofer, Sebastian

DOI: https://doi.org/10.1097/RLI.0000000000000391

Modified Dual-Energy Algorithm for Calcified Plaque Removal
Evaluation in Carotid Computed Tomography Angiography and Comparison With Digital Subtraction Angiography

Manoj Mannil, MD, MSc, Jaychandran Ramachandran, MD,†‡ Ilaria Vittoria de Martini, MD,*† Susanne Wegener, MD,§ Bernhard Schmidt, PhD,||¶ Thomas Flohr, PhD,|| Bernhard Krauss, PhD,|| Antonios Valavanis, MD,† Hatem Alkadhi, MD, MPH, EBCR,* and Sebastian Winklhofer, MD†*

Objectives: Computed tomography angiography (CTA) is a valuable tool for the assessment of carotid artery stenosis. However, blooming artifacts from calcified plaques might result in an overestimation of the stenosis grade. The aim of this study was to investigate a new dual-energy computed tomography (DECT) technique with a modified 3-material decomposition algorithm for calcium removal in extracranial carotid artery stenosis.

Materials and Methods: In this retrospective, institutional review board-approved study, 30 calcified carotid plaques in 22 patients (15 men; mean age, 73 ± 10 years) with clinical suspicion of stroke were included. Dual-energy computed tomography image data were obtained using second-generation dual-source CT with tube voltages at 80 and 140Sn kVp. Conventional CTA and virtual noncalcium (VNCa) images using the modified DECT algorithm were reconstructed. By assessing spectral characteristics, the modified DECT algorithm allows for a selective removal of calcium independent of blooming. Two independent and blinded readers evaluated subjective image quality, blooming artifacts, amount of (residual) calcification, and performed stenosis measurements according to the North American Symptomatic Carotid Endarterectomy Trial (NASCET) criteria. Differences were tested using a pairwise sign test. Paired sample *t* tests with Bonferroni correction ($P < 0.017$) and Bland-Altman analyses were used to test for differences in carotid stenosis measurements between VNCa and conventional CTA using digital subtraction angiography (DSA) as the standard of reference.

Results: Subjective image quality was similar among conventional CTA and VNCa image data sets ($P = 0.82$), whereas blooming artifacts were significantly reduced in VNCa images compared with conventional CTA ($P < 0.001$). Residual calcifications in VNCa images were absent in 11 (37%), minor in 12 (40%), medium sized in 2 (7%), and large in 5 (17%) arteries. Stenosis measurements differed significantly between VNCa (mean NASCET stenosis: 27% ± 20%) and conventional CTA images (mean NASCET stenosis: 39% ± 16%; $P < 0.001$) and between conventional CTA and DSA (23% ± 16%, $P < 0.001$). No significant differences in stenosis measurements were observed between VNCa and DSA ($P = 0.189$), with narrow limits of agreement (mean difference ±1.96 standard deviations: −4.7%, −35.1%, and 25.7%).

Conclusions: A modified 3-material decomposition DECT algorithm for calcium removal was introduced, which allows for an accurate removal of calcified carotid plaques in extracranial carotid artery disease. The algorithm might overcome the problem of overestimation of calcified stenosis due to blooming artifacts in conventional CTA.

Key Words: carotid artery stenosis, computed tomography, dual energy, algorithm, blooming, calcium, artifacts

(*Invest Radiol* 2017;00: 00–00)

Received for publication March 28, 2017; and accepted for publication, after revision, April 25, 2017.

From the *Institute of Diagnostic and Interventional Radiology, and †Department of Neuroradiology, University Hospital Zurich, University of Zurich, Zurich, Switzerland; ‡Department of Neurosciences, Vikram Hospital, Bangalore, India; §Department of Neurology, University Hospital Zurich, University of Zurich, Zurich, Switzerland; ||Siemens Healthcare GmbH; and ¶Institute of Medical Physics, University Erlangen-Nürnberg, Erlangen, Germany.

Correspondence to: Hatem Alkadhi, MD, MPH, EBCR, Institute of Diagnostic and Interventional Radiology, University Hospital Zurich, Raemistrasse 100, 8091 Zurich, Switzerland. E-mail: hatem.alkadhi@usz.ch.

Conflicts of interest and sources of funding: none declared.

ISSN: 0020-9996/17/0000–0000
DOI: 10.1097/RLI.0000000000000391

Stroke is the fifth leading cause of death in the United States and the leading cause of adult disability.[1] Extracranial internal carotid artery (ICA) atherosclerotic occlusive disease is a common reason for ischemic stroke and responsible for approximately 7% to 18% of all first-time ischemic stroke incidents.[2] Although digital subtraction angiography (DSA) is considered the diagnostic reference standard, it is invasive and associated with periprocedural risks.[3]

Computed tomography angiography (CTA) of the cervical vessels is established as an integral part in the imaging workup of acute ischemic stroke. It assesses potential causes of thromboembolic sources and is characterized by a high sensitivity and a high negative predictive value for the assessment of extracranial carotid disease.[3] Computed tomography angiography stenosis measurements demonstrated the best performance at mild stenosis and full carotid occlusion[4]; however, diagnosis of higher stenosis grades with CTA may be hampered by calcified plaques.[5] Calcified plaques may result in an overestimation of the actual stenosis grade because of blooming artifacts. In addition, dense calcium deposits may cause streak and beam hardening artifacts.

Advances in dual-energy CT (DECT)–related material decomposition may allow to overcome this problem: DECT has the ability to differentiate between iodine and calcium contents by using differences in energy dependence of CT attenuation.[5–9] Previous studies have compared the efficiency of plaque and bone removal in DECT angiography of cervical vessels with that of conventional CTA and have found advantages for DECT regarding a reduction of reading time and radiation dose.[6,10–13] Other studies have reported the feasibility and utility of bone and plaque removal in intracranial and cervical DECT angiography examinations compared with DSA[14,15] and the accurate classification of hemorrhagic and calcified cerebral lesions.[16]

Recently, a novel modified DECT material differentiating algorithm was introduced, which is intended to improve the removal of calcified plaques, whereas intraluminal iodine-based contrast and soft tissues are not affected by postprocessing.[17] Instead of using a fixed CT value threshold for the removal of calcifications, which are known to be limited due to calcium blooming, the spectral characteristics are assessed. Using the fact that calcium blooming is present in both high- and low-energy images, the evaluation of spectral behavior allows for the removal of the (bloomed) calcium, leaving images without calcium contributions, and thus allowing for lumen assessment being not impacted by blooming.

We hypothesized that this algorithm would allow for a more accurate evaluation of carotid stenosis in comparison to conventional CTA using DSA as the reference standard. Thus, the aim of this study was to investigate the value of the modified DECT algorithm for an optimized evaluation of carotid artery stenosis.

MATERIALS AND METHODS

Patient Selection

In this retrospective cohort study, we included 22 patients (15 men, 7 women; mean age, 73 ± 10 years; range 51–92 years) with 30 calcified carotid artery stenoses (located either in the carotid bulb or in the proximal ICA).

We screened all patients who presented to our hospitals' emergency department between 2014 and 2016 using the search option of our in-house radiology information system. Included patients had a clinical suspicion of acute stroke and received both a DECT angiography and DSA examination. The DECT scan was performed according to our local stroke protocol consisting of a nonenhanced brain CT, followed by a CTA of the cervical and intracranial vessels performed with dual-energy, a brain perfusion CT, and a contrast-enhanced CT of the brain. Thereafter, DSA of the cervical and intracranial vessels was performed for either diagnostic or therapeutically purposes within 24 hours of initial CT. Patients without calcified carotid stenosis were excluded. Detailed patient information can be found in Table 1.

The study had institutional review board approval. All procedures were performed in accordance with local and federal regulations and the Declaration of Helsinki. The retrospective study was approved by the local ethics committee.

CT Data Acquisition and Postprocessing

Computed tomography angiography data acquisition was performed using a second-generation 128-slice dual-source CT scanner (SOMATOM Definition Flash; Siemens Healthcare GmbH, Erlangen, Germany) in the dual-energy mode. Tube voltages were set to 80 and 140 kVp, the latter operated with tin (Sn) filtration, and with corresponding quality reference tube current-time products of 222 and 111 mA, respectively, using automated tube current modulation (CAREDose4D). Further scanning parameters were as follows: slice acquisition, 2 × 0.6 × 64 mm by means of a z-flying focal spot; rotation time, 0.5 second; and pitch, 0.9. The average volume CT dose index of the protocol was 11.7 mGy.

TABLE 1. Descriptive Statistics

Mean age, y	All	73 ± 10
	Male	70 ± 12
	Female	76 ± 4.9
Sex	Male	15 (68%)
	Female	7 (32%)
Side	Left side	12 (40%)
	Right side	18 (60%)
Location	CCA	9 (30%)
	ICA	21 (70%)
Amount of calcification, CTA	Small	9 (30%)
	Medium	9 (30%)
	Large	12 (40%)
Amount of calcification, VNCa	No residual	11 (36.7%)
	Minor residual	12 (40%)
	Medium-sized residual	2 (6.7%)
	Large residual	5 (16.7%)
Blooming present	CTA	27 (90%)
	VNCa	3 (10%)
Good diagnostic image quality	CTA	29 (96.7%)
	VNCa	29 (96.7%)
Mean attenuation, HU	CTA	352.17 ± 91.97
	VNCa	306.6 ± 69.21
Mean Stenosis, %	CTA reader 1	39.07 ± 16.22
	CTA reader 2	38.05 ± 15.88
	VNCa reader 1	27.01 ± 20.49
	VNCa reader 2	26.33 ± 20.28
	DSA	22.92 ± 15.56

CCA, common carotid artery; CTA, computed tomography angiography; DSA, digital subtraction angiography; HU, Hounsfield units; ICA, internal carotid artery, VNCa, virtual noncalcium.

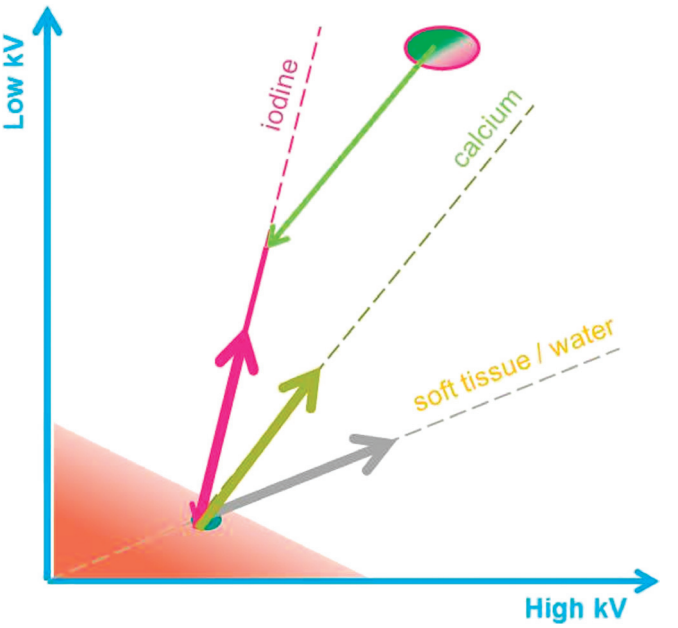

FIGURE 1. Schematic representation of the modified dual-energy CT algorithm. For a complete separation of calcium from iodine-enhanced data sets. Instead of a traditional dual-energy–based material decomposition into iodine at different concentrations and water at different densities, a modified 3-material decomposition into calcium as one base material and a mixture of soft tissue and iodine (by using density constraints) as the other material is performed. Doing so a complete separation of iodine and calcium is performed. Furthermore, challenges of calcium blooming are solved, because not just the calcium itself, but also blooming components are removed due to its spectral behavior, which is unique to calcium.

Patients received 80-mL contrast medium (iobitridol, Xenetics, 350 mg iodine/mL, Guerbet, Gorinchem, the Netherlands) at a flow rate of 5 mL/s. Contrast media was injected over an antecubital vein using a dual-head power injector (Accutron CT-D; Medtron, Saarbrücken, Germany). Computed tomography data acquisition was initiated with bolus tracking via a region of interest in the ascending aorta, using a signal attenuation threshold of 100 Hounsfield units (HU) and a delay of 4 seconds. The scan covered the aortic arch and the vessels and including the circle of Willis.

First, conventional mixed CTA images were reconstructed with a weighting factor of 0.5, representing a mix of images from the low- and high-energy scan resembling single-energy CTA.[18,19] Then, raw data were transferred to an offline workstation (Xeon CPU dual-core 2.8 GHz, 32 GB RAM; Intel, Santa Clara, CA) for postprocessing of virtual noncalcium (VNCa) images using a dedicated prototype software (eXamine, Version 0.9.10; Siemens). A novel, modified postprocessing algorithm was used for calcium removal (see further details hereinafter).

Images from both data sets (conventional CTA and VNCa) were reconstructed with a slice thickness of 0.75 mm, increment of 0.5 mm, using a medium-smooth kernel (D30), a field of view of 250 mm, and an image matrix of 512 × 512. After postprocessing, all image data were transferred for readout to our hospital's picture archiving and communication system (Agfa, Version 6.6.1; Mortsel, Belgium).

Modified DECT Algorithm

Traditional virtual noncontrast imaging algorithms decompose high- and low-energy images into 2 base material images, for example,

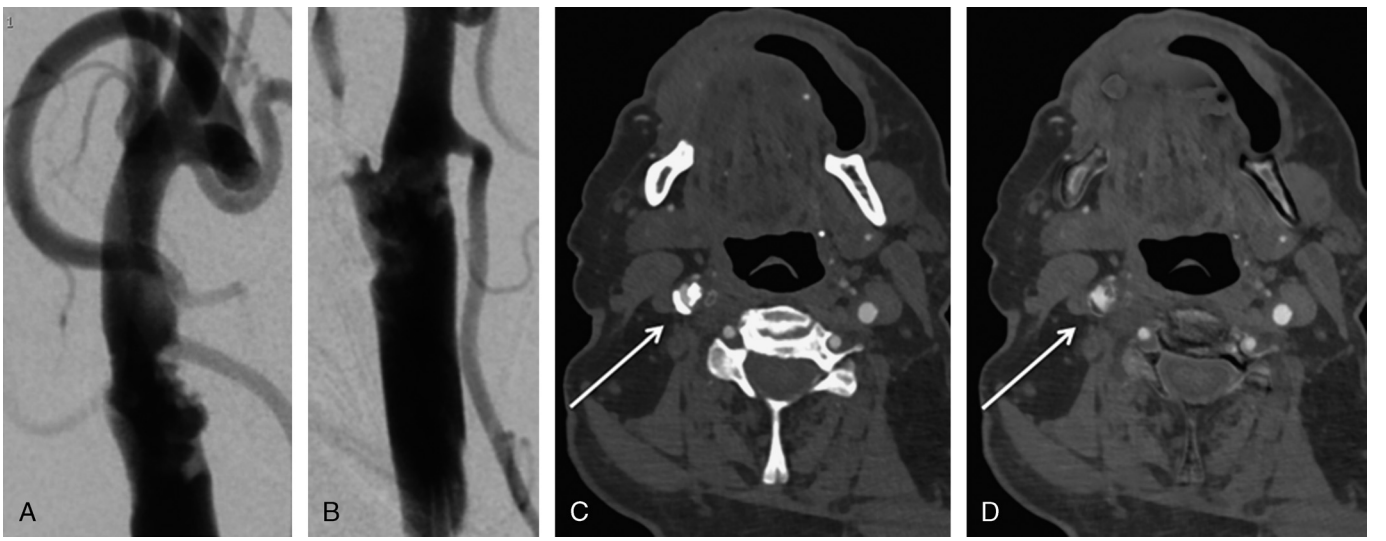

FIGURE 2. A 74-year-old man with calcified stenosis (22%) of the right common carotid artery. A and B, Digital subtraction angiography in coronal and sagittal projection. C and D, Axial mean computed tomography angiography (left) versus axial virtual noncalcium imaging (right) at the location of maximum calcified carotid artery stenosis (arrow).

soft tissue and iodine. In case of the presence of fat, soft tissue can be replaced by a mixture of fat and soft tissue by using a density constraint, which is then called 3-material decomposition. In both scenarios, calcium—being none of the 2 base materials—remains in both images. The iodine image therefore still contains calcium. To allow for a complete removal of calcium, the 3-material decomposition has to be further refined, because specifically iodine and calcium have to be separated completely. Therefore, we decompose the high- and low-kilovolt images into calcium as 1 of the 2 base materials and into a mixture of soft tissue and iodine—while maintaining the CT values of fat and air—as a second base material. Theoretically, this method should allow for a complete removal of calcium (Fig. 1). Hereby, the limitation of calcium blooming is overcome because the blooming of calcium has the spectral characteristic of calcium and is removed as well.[13] To avoid an excessive increase in image noise, a frequency split-based noise reduction method is used.[14] The resulting images are hereafter called *virtual noncalcium* (VNCa) images. Two representative examples of calcified carotid stenosis in DSA, conventional CTA and VNCa images, are depicted in Figures 2 and 3.

Digital Subtraction Angiography

Digital subtraction angiography was performed on a C-arm angiography system with flat panel detectors (Artis zeego; Siemens Healthcare GmbH, Erlangen, Germany). The fluoroscope was operated in the automatic mode for control of tube peak kilovoltage kVp, Cu filtration thickness, and milliamperes. Digital subtraction angiography was performed by 3 experienced interventional neuroradiologists.

Image Analysis

Both CT image data sets (conventional CTA and VNCa) were independently analyzed twice by the same reader with a time interval of 2 weeks for determining intrareader reliability (R1, board-certified

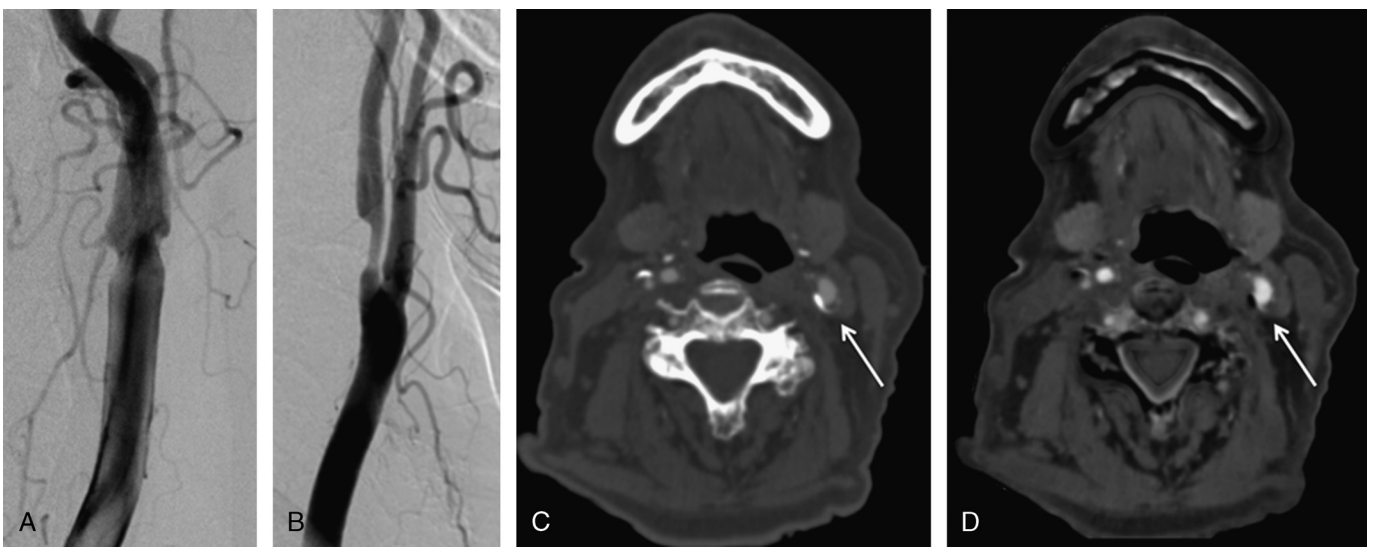

FIGURE 3. A 78-year-old woman with mixed plaque stenosis (59%) of the left internal carotid artery. A and B, Digital subtraction angiography in coronal and sagittal projection. C and D, Axial mean computed tomography angiography (left) versus axial virtual noncalcium imaging (right) at the location of maximum calcified carotid artery stenosis (arrow).

TABLE 2. Intrareader and Interreader Agreement

	Intrareader ICC	Interreader ICC
CTA stenosis measurements	0.97	0.98
VNCa stenosis measurements	0.99	0.98
	Intrareader γ	**Interreader γ**
Image quality CTA	1	1
Image quality VNCa	1	1
Blooming CTA	0.96	1
Blooming VNCa	1	1
VNCa amount of residual calcification	0.77	0.987

CTA, computed tomography angiography; ICC, intraclass correlation coefficient; VNCa, virtual noncalcium.

neuroradiologist with 8 years of experience in neuroradiology). A second reader (R2, with 4 years of experience in neuroradiology) analyzed the image data sets a third time for determining interreader reliability. Both readers were blinded to the results from DSA.

Digital subtraction angiography reference measurements were performed in consensus by R1 and a board-certified neurologist (R3, with 5 years of experience in stroke imaging), both being blinded to the results from CT.

Qualitative Readout

Overall image quality of conventional CTA and VNCa images was assessed using a subjective 3-point Likert scale (1 = excellent, 2 = moderate, still diagnostic, 3 = insufficient, nondiagnostic). The assessment of intraluminal blooming artifacts was dichotomized to be "present" or "absent". The amount of calcification in CTA and VNCa images was assessed using a 3-point Likert scale (1 = small, 2 = medium, 3 = large).

Residual calcifications in VNCa images in comparison to conventional CTA images were graded using a 5-point Likert scale (1 = none, 2 = minor, 3 = medium, 4 = large, 5 = no difference between VNCa and conventional CTA).

Quantitative Readout

Stenosis measurements of the common carotid artery and the extracranial portions of the ICA in DSA, conventional CTA, and VNCa were performed according to the North American Symptomatic Carotid Endarterectomy Trial (NASCET).[20] The ratio between the residual luminal diameter (inner-to-inner lumen) and the diameter of a distal reference lumen (inner-to-inner lumen) were calculated according to $\frac{\text{Reference diameter} - \text{Stenosis diameter}}{\text{Reference diameter}} 100\,\%$. Computed tomography angiography and VNCa stenosis measurements were performed on multiplanar reformations. Stenoses of the external carotid artery were not analyzed due to branching and due to the lack of clinical relevance.

Mean intraluminal attenuation values (Hounsfield units) were measured in matched locations of conventional CTA and VNCa image data using a standardized circled region of interest in the extracranial portion of the ICA distal to the stenosis.

Statistical Analysis

Continuous variables were expressed as means ± standard deviation, and categorical variables as frequencies or percentages. The intrareader and interreader agreement regarding quantitative stenosis measurements were analyzed by using intraclass correlation coefficients (ICCs). The intrareader and interreader agreement for qualitative imaging parameters (image quality, blooming artifacts, and amount of calcifications) was calculated by using Goodman and Kruskal's gamma. According to Landis and Koch,[21] values of 0.61 to 0.80 were interpreted as substantial, and 0.81 to 1.00, as excellent agreement.

Differences in the presence of blooming artifacts between conventional CTA and VNCa images were tested using a pairwise sign test. After confirming normal distribution of continuous stenosis measurements using the Shapiro-Wilk test, paired sample *t* tests with Bonferroni correction were used to account for differences between conventional CTA, VNCa, and DSA stenosis measurements. Differences in stenosis measurements between DSA and VNCa were further analyzed using the method of Bland-Altman.[22] A Pearson correlation was performed between the stenosis in DSA and the absolute error (VNCa stenosis − DSA stenosis) in VNCa images.

Nonnormally distributed mean attenuation values in VNCa and conventional CTA were compared using a Wilcoxon-signed rank test. If not stated otherwise, a 2-tailed *P* value below 0.05 indicated statistical significance. All statistical analyses were conducted using commercially available software (SPSS, release 23.0; IBM, Chicago, IL).

RESULTS

Intrareader and Interreader Agreement

NASCET carotid artery stenosis measurements yielded excellent ICC values of 0.97 (intrareader) and 0.98 (interreader) for conventional CTA, and 0.99 and 0.98, respectively, for VNCa. Assessment of residual calcifications in VNCa yielded substantial to excellent ICC values of 0.79 (intrareader) and 0.81 (interreader) (Table 2).

Qualitative Results

Excellent image quality was observed in 29 (97%) of 30 of arteries for both conventional CTA and VNCa images (see Figures 2 and 3). The single patient with insufficient, nondiagnostic image quality showed streak artifacts from metallic dental prostheses in both CTA and VNCa images. The calcium removal tool was nonfunctional in this case, and the stenosis measurements in VNCa images were identical to those using CTA images.

Blooming artifacts were present in 27 (90%) of 30 arteries on conventional CTA images and were significantly reduced to 3 (10%) of 30 arteries in VNCa images ($P < 0.001$) The amount of calcification causing the stenosis in conventional CTA was small in 9 (30%), medium in 9 (30%), and large in 12 (40%) arteries. Residual calcifications in VNCa images at the site of stenosis were absent in 11 (37%), minor in 12 (40%), medium sized in 2 (7%), and large in 5 (17%) arteries (Table 1).

TABLE 3. Comparison of CTA, VNCa, and DSA Stenosis Measurements

Stenosis 1, %	Mean 1 ± SD	Stenosis 2, %	Mean 2 ± SD	*P* (Stenosis 1 vs 2)
CTA	39.07 ± 16.22	vs DSA	22.92 ± 15.56	<0.001
VNCa	27.01 ± 20.49	vs DSA	22.92 ± 15.56	0.189
CTA	39.07 ± 16.22	vs VNCa	27.01 ± 20.49	<0.001

CTA, computed tomography angiography; DSA, digital subtraction angiography; SD, standard deviation; VNCa, virtual noncalcium.

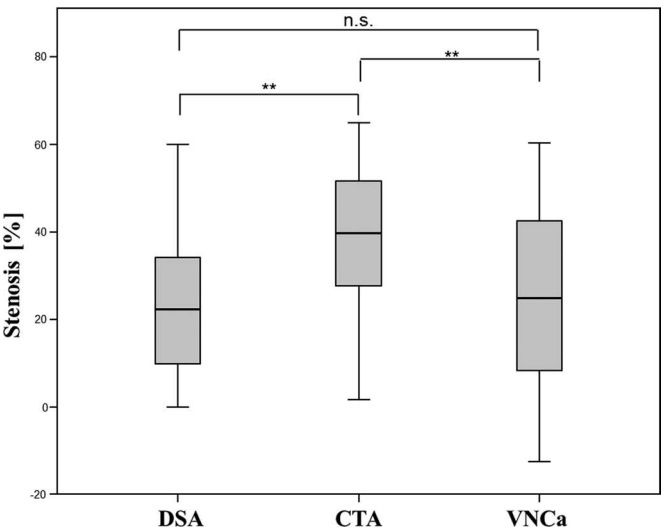

FIGURE 4. Box whisker plot illustrating differences in extracranial carotid artery stenosis measurements between digital subtraction angiography and mean computed tomography angiography. Boxes indicate 25th and 75th percentiles. Horizontal line indicates median value (50th percentile). Brackets include minimum and maximum nonextreme values.

Quantitative Results

According to the reference standard DSA, mean carotid artery stenosis was 23% ± 16%. Stenoses in conventional CTA were 39% ± 16% and 27% ± 21% for VNCa (Table 3). Significant differences were observed between conventional CTA and DSA ($P < 0.001$), between conventional CTA and VNCa ($P < 0.001$), but no differences were found between VNCa and DSA ($P = 0.189$) (Fig. 4). NASCET stenosis measurements (%) on DSA and VNCa images showed a small mean error (−4.7) and narrow limits of agreement (−35.1; 25.7) (Fig. 5). No systematic bias was observed. There was no significant correlation between the absolute stenosis in DSA and the absolute error (VNCa stenosis − DSA stenosis) on VNCa images ($r = 0.21$, $P = 0.27$) indicating no relationship between the extent of stenosis and success of calcified plaque removal.

Mean intraluminal attenuation of the extracranial portion of the ICA was 352 ± 92 HU in CTA images. Mean intraluminal attenuation at matched locations was significantly ($P < 0.001$) lower for VNCa with 307 ± 6 HU (mean difference, 45 HU).

DISCUSSION

This study introduces a novel modified DECT algorithm, which allows for removal of calcifications being not impacted by calcium blooming. Our study indicates that this modified DECT algorithm allows for a removal of calcified carotid vessel wall plaques and thus for an improved quantification of carotid artery stenosis being better than that using conventional CTA images, and with similar results as compared with the criterion standard modality DSA.

Dual-energy computed tomography is characterized by the acquisition of 2 image sets at 2 different x-ray spectra. There are 2 main mechanisms responsible for material-dependent attenuation differences: (1) Compton scatter and (2) photoelectric effect. The latter is strongly depending on the atomic number of the investigated material, whereas the first depends more on irradiated tissue size, beam quality, and beam energy. Based on these characteristics, DECT enables the differentiation between various materials with high atomic numbers, such as iodine and calcium. The modified algorithm introduced herein applies a 3-material

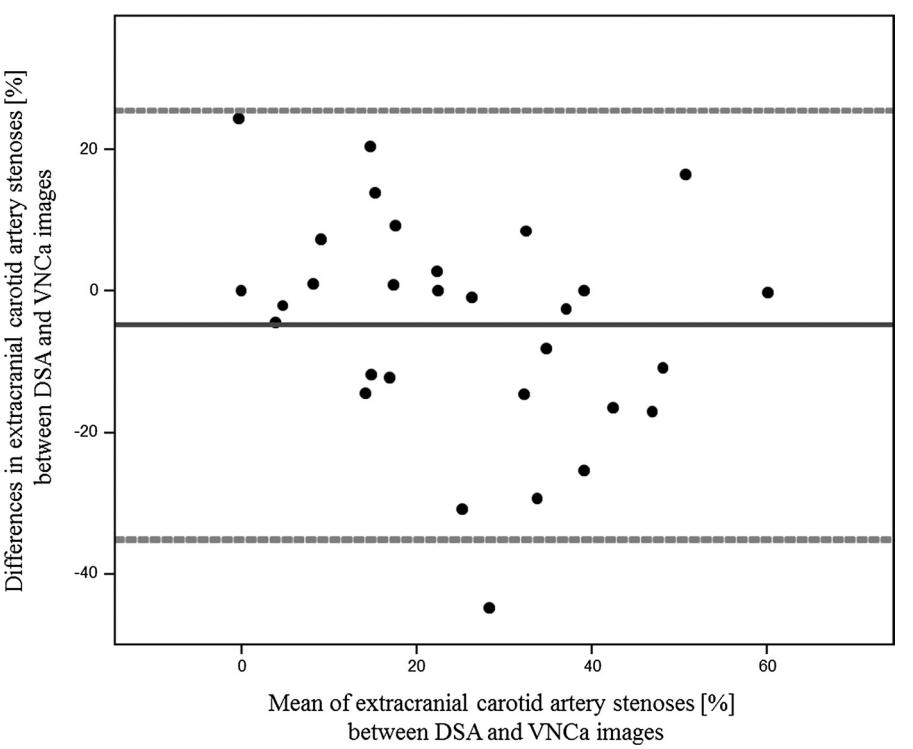

FIGURE 5. Bland-Altman plot comparing absolute NASCET stenosis measurements (%) of digital subtraction angiography and virtual noncalcium imaging. The horizontal center line indicates mean difference between DSA and VNCa stenosis measurements. Dashed lines indicate upper and lower margins of 95% confidence interval (±1.96 SD). The single outlier below the lower margin represents the case of nondiagnostic image quality due to artifacts from dental prosthesis. Figure 5 can be viewed online in color at www.investigativeradiology.com.

decomposition technique into calcium as one material and a mixture out of soft tissue and iodine as the other material. This enables the complete removal of calcium and avoids residual amounts of calcium in iodine images.

A few studies so far have investigated the usefulness of DECT angiography for depiction of cervical arteries.[6,12,14,23,24] For example, Morhard et al[6] used DECT for removing bone (ie, the skull base) from images for an improved carotid vessel delineation. Similarly, Lell et al[12] and Kaemmerer et al[13] used DECT for subtraction of skull base bone in carotid angiography and showed a good visualization of vessels devoid of overlaid bone. Uotani et al[14] performed DECT and removed calcium in carotid artery stenosis using an early-stage 2-material decomposition algorithm and showed a decrease in false-positive carotid artery stenosis rates in comparison to conventional CTA. They were using maximum intensity projection images, which are known to resemble DSA-like images. However, stenosis measurements are not reliable on maximum intensity projection images as ring-like calcifications in the arterial wall can mask the perfused lumen.[4]

With the modified DECT algorithm, calcified plaques were sufficiently removed in the majority (97%) of arteries in most (95%) of our patients, resulting in a significant reduction of blooming artifacts while preserving the image quality of the VNCa images. Even in the rare cases of medium or large residual calcifications in VNCa images, NASCET stenosis measurements were on average 9% smaller compared with those using conventional CTA images. Based on the VNCa images with largely removed plaques (and hence, reduced blooming artifacts), quantitative stenosis grading was possible, yielding results that were significantly lower as compared with those from conventional CTA. This indicates that plaque removal with the modified DECT algorithm also reduced the issue of blooming artifacts, which is known to lead to an overestimation of stenosis severity. This is further corroborated by the fact that stenosis grading on VNCa images were similar to those from the criterion standard modality DSA, whereas measurements based on conventional CTA images significantly overestimated stenosis grades. The nonsignificant correlation between absolute stenosis in DSA and the absolute error in VNCa images indicates that the modified 3-material decomposition DECT algorithm is working voxel-wise and independent of the stenosis severity.

While calcium removal was feasible in 97% of arteries, it failed in 1 artery, with insufficient, nondiagnostic image quality due to metallic dental prostheses, which indicates that the algorithm has limitations in its current form. Furthermore, we observed significantly lower intraluminal attenuation values in VNCa compared with conventional CTA images. This suggests that the modified DECT calcium removal algorithm may partially remove iodine as well due to calibration tolerances of the base material decomposition.

The following study limitations must be acknowledged. First, this was a retrospective study with inherent limitations. Second, we included a relatively low number of individuals and no patients had severe stenosis. However, this study represents the first proof of principle with robust results on a novel calcium removal algorithm for DECT. General inferences on the limitations of the algorithm need to be validated in larger, prospective trials. Finally, we did not directly compare the novel modified DECT algorithm with previous nonmodified calcium removal DECT techniques.

In conclusion, our study demonstrates the feasibility of a novel 3-material decomposition DECT algorithm for calcium removal in extracranial carotid artery disease. This technique might overcome previous problems of overestimating stenosis severity due to blooming artifacts from calcified plaques in CTA.

REFERENCES

1. Writing Group M, Mozaffarian D, Benjamin EJ, et al. Heart disease and stroke statistics-2016 update: a report from the American Heart Association. *Circulation*. 2016;133:e38–e360.
2. Barrett KM, Brott TG. Stroke caused by extracranial disease. *Circ Res*. 2017;120:496–501.
3. Josephson SA, Bryant SO, Mak HK, et al. Evaluation of carotid stenosis using CT angiography in the initial evaluation of stroke and TIA. *Neurology*. 2004;63:457–460.
4. Silvennoinen HM, Ikonen S, Soinne L, et al. CT angiographic analysis of carotid artery stenosis: comparison of manual assessment, semiautomatic vessel analysis, and digital subtraction angiography. *AJNR Am J Neuroradiol*. 2007;28:97–103.
5. Thomas C, Korn A, Ketelsen D, et al. Automatic lumen segmentation in calcified plaques: dual-energy CT versus standard reconstructions in comparison with digital subtraction angiography. *AJR Am J Roentgenol*. 2010;194:1590–1595.
6. Morhard D, Fink C, Graser A, et al. Cervical and cranial computed tomographic angiography with automated bone removal: dual energy computed tomography versus standard computed tomography. *Invest Radiol*. 2009;44:293–297.
7. Krauss B, Grant KL, Schmidt BT, et al. The importance of spectral separation: an assessment of dual-energy spectral separation for quantitative ability and dose efficiency. *Invest Radiol*. 2015;50:114–118.
8. Lambert JW, Sun Y, Gould RG, et al. An image-domain contrast material extraction method for dual-energy computed tomography. *Invest Radiol*. 2017;52:245–254.
9. Runge VM, Marquez H, Andreisek G, et al. Recent technological advances in computed tomography and the clinical impact therein. *Invest Radiol*. 2015;50:119–127.
10. Deng K, Liu C, Ma R, et al. Clinical evaluation of dual-energy bone removal in CT angiography of the head and neck: comparison with conventional bone-subtraction CT angiography. *Clin Radiol*. 2009;64:534–541.
11. Thomas C, Korn A, Krauss B, et al. Automatic bone and plaque removal using dual energy CT for head and neck angiography: feasibility and initial performance evaluation. *Eur J Radiol*. 2010;76:61–67.
12. Lell MM, Kramer M, Klotz E, et al. Carotid computed tomography angiography with automated bone suppression: a comparative study between dual energy and bone subtraction techniques. *Invest Radiol*. 2009;44:322–328.
13. Kaemmerer N, Brand M, Hammon M, et al. Dual-energy computed tomography angiography of the head and neck with single-source computed tomography: a new technical (Split Filter) approach for bone removal. *Invest Radiol*. 2016;51:618–623.
14. Uotani K, Watanabe Y, Higashi M, et al. Dual-energy CT head bone and hard plaque removal for quantification of calcified carotid stenosis: utility and comparison with digital subtraction angiography. *Eur Radiol*. 2009;19:2060–2065.
15. Watanabe Y, Uotani K, Nakazawa T, et al. Dual-energy direct bone removal CT angiography for evaluation of intracranial aneurysm or stenosis: comparison with conventional digital subtraction angiography. *Eur Radiol*. 2009;19:1019–1024.
16. Nute JL, Jacobsen MC, Chandler A, et al. Dual-energy computed tomography for the characterization of intracranial hemorrhage and calcification: a systematic approach in a phantom system. *Invest Radiol*. 2017;52:30–41.
17. Krauss B, Grant K, Allmendinger T, et al. *Modified dual energy-based three material decomposition for calcium plaque removal without compromising iodine contrast*. Chicago: RSNA; 2016.
18. Yu L, Primak AN, Liu X, et al. Image quality optimization and evaluation of linearly mixed images in dual-source, dual-energy CT. *Med Phys*. 2009;36:1019–1024.
19. Behrendt FF, Schmidt B, Plumhans C, et al. Image fusion in dual energy computed tomography: effect on contrast enhancement, signal-to-noise ratio and image quality in computed tomography angiography. *Invest Radiol*. 2009;44:1–6.
20. North American Symptomatic Carotid Endarterectomy Trial Collaborators, Barnett HJM, Taylor DW, Haynes RB. Beneficial effect of carotid endarterectomy in symptomatic patients with high-grade carotid stenosis. *N Engl J Med* 1991;325:445–453.
21. Landis JR, Koch GG. The measurement of observer agreement for categorical data. *Biometrics*. 1977;33:159–174.
22. Bland JM, Altman DG. Statistical methods for assessing agreement between two methods of clinical measurement. *Lancet*. 1986;1:307–310.
23. Korn A, Bender B, Schabel C, et al. Dual-source dual-energy CT angiography of the supra-aortic arteries with tin filter: impact of tube voltage selection. *Acad Radiol*. 2015;22:708–713.
24. Schneider D, Apfaltrer P, Sudarski S, et al. Optimization of kiloelectron volt settings in cerebral and cervical dual-energy CT angiography determined with virtual monoenergetic imaging. *Acad Radiol*. 2014;21:431–436.